Influence of material anisotropy on the interaction between cracks under tension and shear

A.V. Savikovskii [iD] [1,2] ✉, **A.S. Semenov** [iD] [1]

[1] Peter the Great St. Petersburg Polytechnic University, St. Petersburg, Russia

[2] JSC «Power machines», St. Petersburg, Russia

✉ savikovskii.artem@yandex.ru

Abstract. The fracture of anisotropic bodies with multiple macrocraks is analyzed by means of modeling interaction between cracks and interaction of crack with the free boundary. The influence of material anisotropy on cracks behavior is investigated for orthotropic material, material with cubic symmetry and isotropic material. Article deals with numerical computations of stress intensity factors of internal and edge cracks in the rectangular plate under uniaxial tension and pure shear loadings. The displacement extrapolation method is used for the computation of stress intensity factors for anisotropic materials. The effect of material anisotropy on stress intensity factors for different crack configurations (one, two and three cracks of different lengths) under various loading conditions (tension or shear) is investigated and discussed.

Keywords: linear elastic fracture mechanics; anisotropic material; stress intensity factor; finite-element modeling; displacement extrapolation method; Lekhnitskii formalism, crack

Introduction

Single-crystal nickel-based superalloys [1] are widely used for production of blades of gas turbine engines [2]. These materials have a pronounced anisotropy (cubic symmetry) and temperature dependence of mechanical properties [2]. Cracking of the gas turbine blades is caused by fatigue, creep and thermal fatigue and also corrosion [3–8]. The stress intensity factor (SIF) is the most widespread parameter in the linear fracture mechanics that defines stress state near the crack tip and is used for crack propagation prediction. Determination of SIF for the isotropic material is extensively studied in details theoretically and numerically [9–13] et al., while the study of cracks in anisotropic solids has received much less attention [14–16].

Effects of delay time, crystallographic orientation and mechanical properties of single-crystal anisotropic superalloys on the number of cycles to the main crack formation in thermal fatigue experiments were investigated in paper [17]. Effect of material anisotropy on the crack interaction with a free boundary for the central crack for I fracture mode and the central inclined crack in the finite plate under mixed mode was investigated in paper [18]. Effect of crack orientation with respect to material anisotropy axes on SIF for the anisotropic finite plane was studied in paper [19]. Effect of free edge and material axes orientation on SIF in anisotropic

CT-sample was studied in paper [20]. However, determination of SIF in conditions of mutual influence of cracks and material anisotropy is more complex and less studied. The paper deals with edge cracks in anisotropic bodies and consider the influence of (i) the material anisotropy, (ii) the number of cracks and (iii) the distance from the free boundary on SIFs.

The analytical solutions for SIFs concerning the *single internal inclined crack* in the infinite plane under uniaxial tension for both isotropic and anisotropic materials are defined by relations [14]:

$$K_I = \sigma_\infty \sqrt{\pi l}\, \sin^2\varphi, \qquad K_{II} = \sigma_\infty \sqrt{\pi l}\, \sin\varphi\cos\varphi, \tag{1}$$

where σ_∞ is the value of uniform tensile stress at infinity, l is the half-length of the crack, φ is the angle between the crack and of the uniaxial tensile stress direction. Note, that the analytical solution is the same for isotropic and anisotropic material. Handbook [12] points to the solutions for one, two and three edge cracks in the infinite isotropic half-plane under uniaxial tension.

SIFs for the *single edge crack* is defined by expressions:

$$K_I = 1.1215\sigma_\infty \sqrt{\pi l}, \qquad K_{II} = 0, \tag{2}$$

where σ_∞ is the value of tensile stress, l is the length of the crack. This solution is depended (in contrast to (1)) on material anisotropy even for infinite half-plane. Coefficients 1.1215 and 0 are valid for the isotropic material only. Due to the symmetry of the problem, a pure I mode with $K_{II} = 0$ is realized in the isotropic material.

SIFs for *two edge horizontal cracks* (of equal lengths l and with a distance between cracks also equal to l) in infinite isotropic half-plane are defined by relations:

$$K_I = 0.854\sigma_\infty \sqrt{\pi l}, \qquad K_{II} = 0.1333\sigma_\infty \sqrt{\pi l}. \tag{3}$$

This solution is depended on material anisotropic properties. Coefficients 0.854 and 0.1333 correspond to isotropic material only. The mutual influence of cracks gives rise to the appearance of a mixed fracture mode and the appearance of nonzero K_{II}.

SIFs for *three edge horizontal cracks* (of equal lengths l and with a distance between cracks also equal to l) in isotropic half-plane are defined by expressions (for outside cracks):

$$K_I = 0.815\sigma_\infty \sqrt{\pi l}, \qquad K_{II} = 0.590\sigma_\infty \sqrt{\pi l}. \tag{4}$$

Solution (4) is also sensitive to the material anisotropy. Specified coefficients 0.815 and 0.590 correspond to the isotropic material.

Studying of material anisotropy effect on the interaction between cracks for the finite bodies represents important problem for the reliability analysis of real industrial structures. Application of analytical methods for the general case of arbitrary configurations of multiple cracks is significantly limited, therefore, numerical methods for calculating the SIF are used.

Fracture problem formulations

The four problems with various crack configurations are considered: a single internal central crack in the rectangular plate (Fig. 1); a single edge crack in the rectangular plate (Fig. 2); two edge cracks in the rectangular plate (Fig. 3); three edge cracks in the rectangular plane (Fig. 4). In each of the four tasks listed above, two loading options were considered: uniaxial tension in vertical direction (Figs. 1(a), 2(a), 3(a), 4(a)); pure shear loading (Figs. 1(b), 2(b), 3(b), 4(b)).

The problems are solved in two-dimensional formulation under assumption of plane stress state. Isotropic and anisotropic materials are considered and compared. Anisotropy axes are parallel to edges of plate and global coordinate axes. Studying of material anisotropy effect is carried out using multivariant computations with varied sizes of the plate. Calculation of SIFs has been performed by means of the finite element program PANTOCATOR [21], which has the ability of automatized SIF calculations for isotropic and anisotropic materials based on various numerical methods. Thus anisotropy, dimensions of the plate and fracture modes are varied in the calculation process. In all computations tensile stress σ_∞ is equal to 100 MPa and shear stress τ_∞ is also equal to 100 MPa.

(a)   (b)

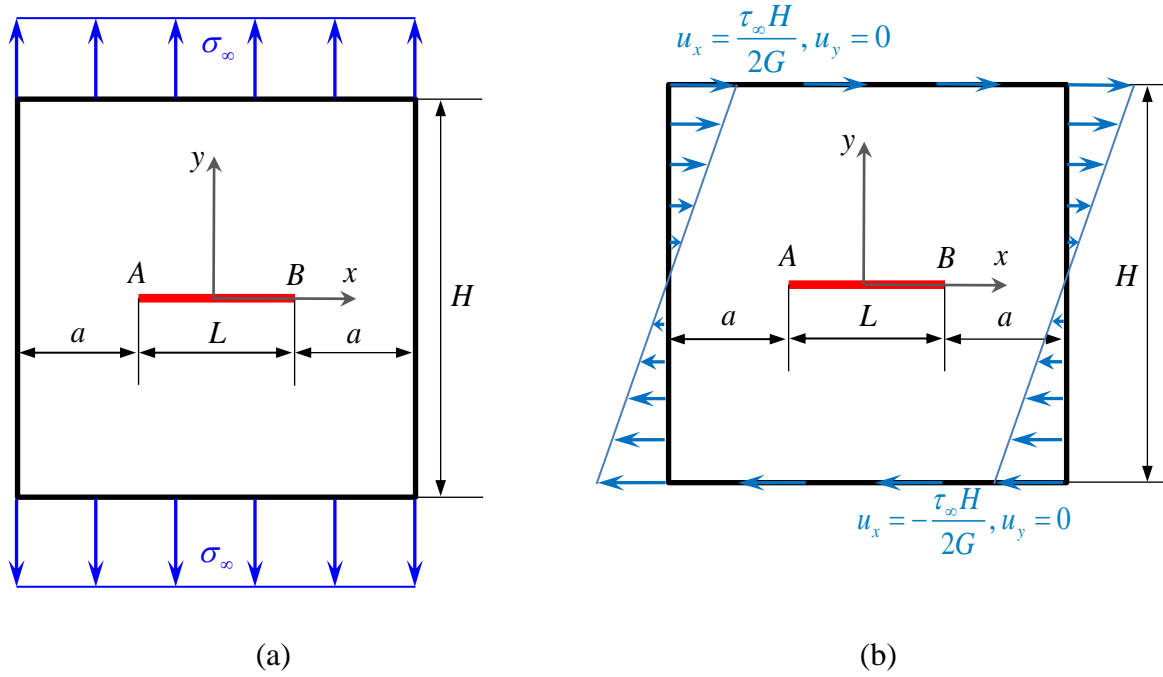**Fig. 1.** Single internal central crack in the rectangular plate under
(a) tension (I fracture mode), and (b) shear (II fracture mode)

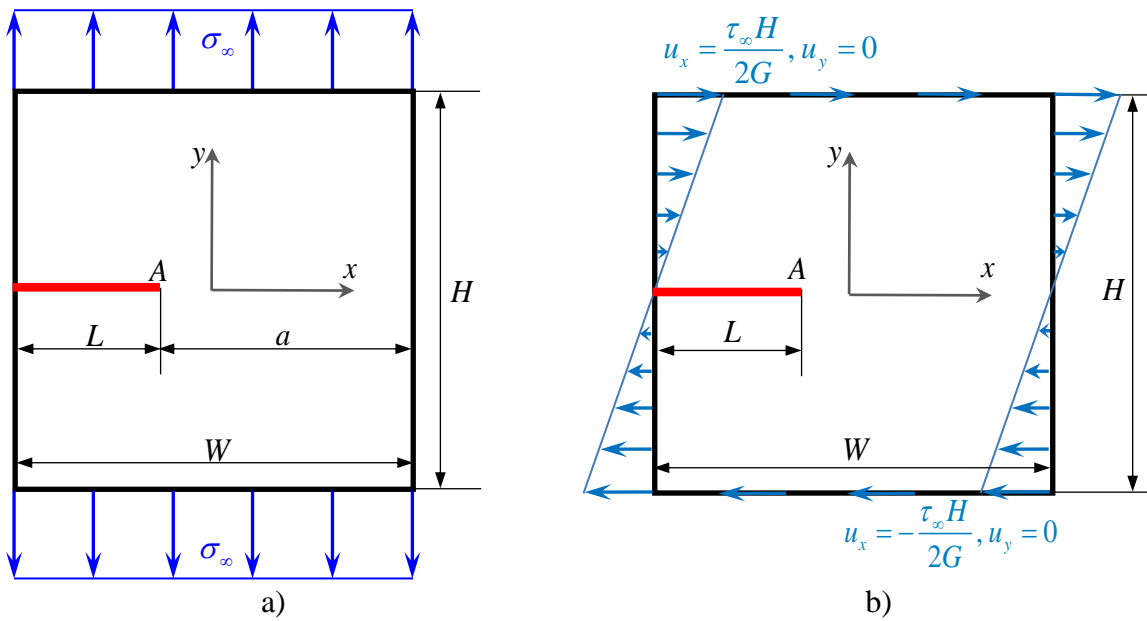a)   b)

Fig. 2. Single edge crack in the rectangular plate under
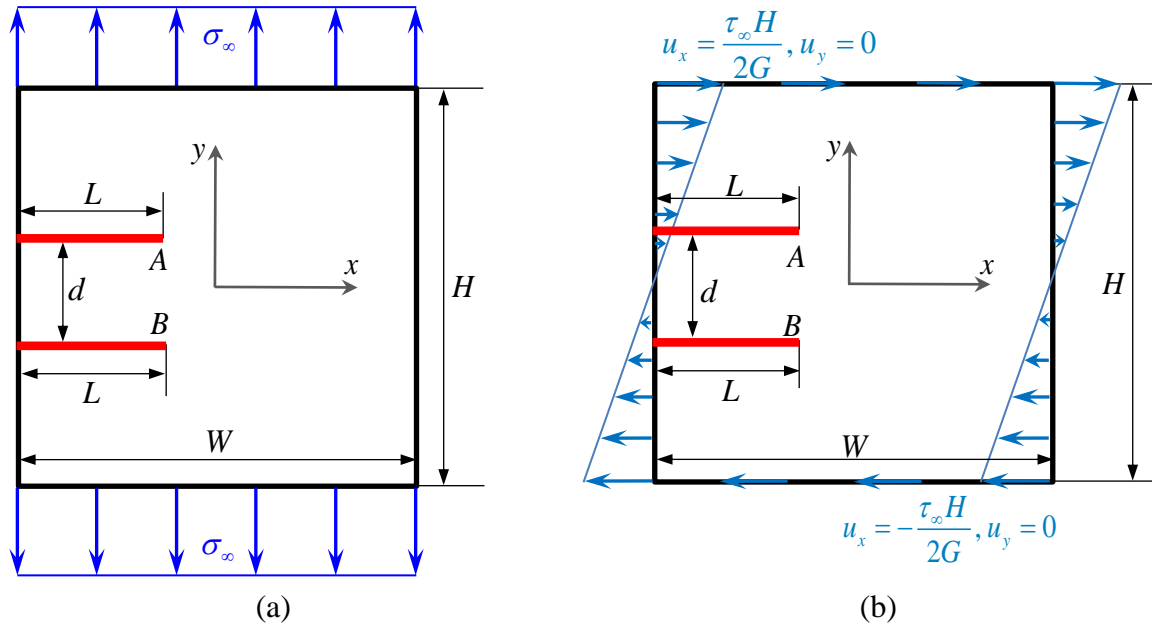(a) tension (I fracture mode), (b) shear (II fracture mode)

Fig. 3. Two edge cracks in the rectangular plate under (a) tension, and (b) shear
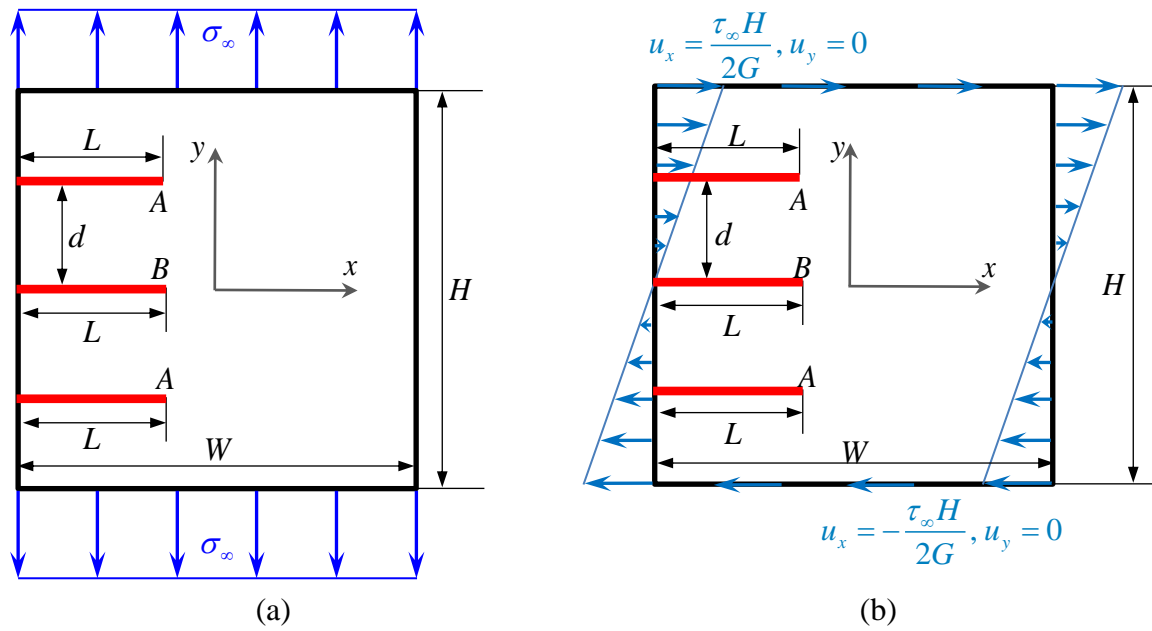

Fig. 4. Three edge cracks in the rectangular plate under (a) tension, and (b) shear

Table 1. Elastic moduli used in computations

Material	Young's modulus, MPa	Shear modulus, MPa	Poisson ratio
Isotropic material	$E = 20000$	$G = 7692.3$	$v = 0.3$
Cubic symmetry, $\rho = -0.25$	$E = 20000$	$G = 200000$	$v = 0.3$
Cubic symmetry, $\rho = -0.17$	$E = 20000$	$G = 77000$	$v = 0.3$
Cubic symmetry, $\rho = 0.37$	$E = 20000$	$G = 15000$	$v = 0.3$
Cubic symmetry, $\rho = 10$	$E = 20000$	$G = 970.8$	$v = 0.3$
Orthotropic material 1	$E_1 = 100000$ $E_2 = 20000$	$G_{12} = 970.8$	$v_{12} = 0.3$
Orthotropic material 2	$E_1 = 6000$ $E_2 = 20000$	$G_{12} = 970.8$	$v_{12} = 0.3$

For each of the four boundary value problems (see Figs. 1-4), three classes of anisotropy were considered to study the effect of anisotropy on crack behavior: isotropic material, material with cubic symmetry, and orthotropic material. Material properties used in computations are summarized in Table 1.

In Table 1 the parameter ρ characterized for the cubic symmetry (with three independent elastic moduli E, v, G) the deviation from isotropy:

$$\rho = \frac{E}{2G} - v. \tag{5}$$

For the isotropic material the parameter ρ equal to 1. In computations the value of G varied for fixed values of elastic modules E and v.

Displacement extrapolation method for stress intensity factors calculation

The crack-tip displacement fields in polar coordinates in the general three-dimensional case (nonzero K_I, K_{II}, K_{III}) for an *isotropic* material are given by relations [22]:

$$u_x(r,\alpha) = \frac{K_I}{G}\sqrt{\frac{r}{2\pi}}\cos\frac{\alpha}{2}\left(\frac{\kappa-1}{2}+\sin^2\frac{\alpha}{2}\right)+\frac{K_{II}}{G}\sqrt{\frac{r}{2\pi}}\sin\frac{\alpha}{2}\left(\frac{\kappa+1}{2}+\cos^2\frac{\alpha}{2}\right),$$

$$u_y(r,\alpha) = \frac{K_I}{G}\sqrt{\frac{r}{2\pi}}\sin\frac{\alpha}{2}\left(\frac{\kappa+1}{2}-\cos^2\frac{\alpha}{2}\right)+\frac{K_{II}}{G}\sqrt{\frac{r}{2\pi}}\cos\frac{\alpha}{2}\left(\frac{\kappa-1}{2}+\sin^2\frac{\alpha}{2}\right), \tag{6}$$

$$u_z(r,\alpha) = \frac{K_{III}}{G}\sqrt{\frac{r}{2\pi}}\sin\frac{\alpha}{2},$$

where $u_x(r,\alpha), u_y(r,\alpha), u_z(r,\alpha)$ are axial displacements in crack coordinate systems, K_I, K_{II}, K_{III} are SIFs for I, II and III fracture modes, the Kolosov's constant $\kappa = \frac{3-v}{1+v}$ in the case of plane stress state, G is the shear modulus, r is the distance from crack tip to considered point, α is the angle between point direction and crack axis, v is the Poisson's ratio.

Asymptotic expressions for displacements near the crack tip in the general three-dimensional case for *anisotropic* material obtained using the Lekhnitskii formalism have the following form [14, 23, 24]:

$$u_x(r,\alpha) = \frac{K_I\sqrt{2r}}{\sqrt{\pi}}\text{Re}\left(\frac{1}{\mu_1'-\mu_2'}\left(\mu_1'p_2\sqrt{\cos\alpha+\mu_2'\sin\alpha}-\mu_2'p_1\sqrt{\cos\alpha+\mu_1'\sin\alpha}\right)\right)+$$

$$+\frac{K_{II}\sqrt{2r}}{\sqrt{\pi}}\text{Re}\left(\frac{1}{\mu_1'-\mu_2'}\left(p_2\sqrt{\cos\alpha+\mu_2'\sin\alpha}-p_1\sqrt{\cos\alpha+\mu_1'\sin\alpha}\right)\right),$$

$$u_y(r,\alpha) = \frac{K_I\sqrt{2r}}{\sqrt{\pi}}\text{Re}\left(\frac{1}{\mu_1'-\mu_2'}\left(\mu_1'q_2\sqrt{\cos\alpha+\mu_2'\sin\alpha}-\mu_2'q_1\sqrt{\cos\alpha+\mu_1'\sin\alpha}\right)\right)+ \tag{7}$$

$$+\frac{K_{II}\sqrt{2r}}{\sqrt{\pi}}\text{Re}\left(\frac{1}{\mu_1'-\mu_2'}\left(q_2\sqrt{\cos\alpha+\mu_2'\sin\alpha}-q_1\sqrt{\cos\alpha+\mu_1'\sin\alpha}\right)\right),$$

$$u_z(r,\alpha) = \frac{K_{III}\sqrt{2r}}{\sqrt{\pi}}\text{Re}\left(\frac{\sqrt{\cos\alpha+\mu_3'\sin\alpha}}{C_{45}+\mu_3 C_{44}}\right),$$

where μ_1' and μ_2' are the complex-valued roots of the fourth degree equation (complex parameters of anisotropic material [25])

$$S_{11}'\mu^4 - 2S_{16}'\mu^3 + (2S_{12}'+S_{66}')\mu^2 - 2S_{26}'\mu + S_{22}' = 0 \tag{8}$$

with positive imaginary part, $S_{ij}^{'}$ are the elements of the elastic compliance matrix of the material in the crack coordinate system, $p_i = S_{11}^{'}\mu_i^{'2} + S_{12}^{'} - S_{16}^{'}\mu_i^{'}, q_i = S_{12}^{'}\mu_i^{'} + \dfrac{S_{22}^{'}}{\mu_i^{'}} - S_{26}^{'}$, $\mu_3^{'}$ is

the root of equation $C_{44}^{'}\mu^2 - 2C_{45}^{'}\mu + C_{55}^{'} = 0$ with positive imaginary part, $C_{ij}^{'}$ are the constants of the matrix of elastic modules of the material in the crack coordinate system ($[C] = [S]^{-1}$).

In the case of an *isotropic* material, the displacements are related to SIFs by formulas (6). Substitution of $\alpha = \pm\pi$ in the equation (6) leads to the expression for the SIFs in terms of displacement jumps on the crack banks for the isotropic material:

$$K_I = \lim_{r\to 0}\left(\left[u_y(r,\pi) - u_y(r,-\pi) \right]\sqrt{\frac{2\pi}{r}}\frac{G}{1+\kappa} \right),$$

$$K_{II} = \lim_{r\to 0}\left(\left[u_x(r,\pi) - u_x(r,-\pi) \right]\sqrt{\frac{2\pi}{r}}\frac{G}{1+\kappa} \right), \tag{9}$$

$$K_{III} = \lim_{r\to 0}\left(\left[u_z(r,\pi) - u_z(r,-\pi) \right]\sqrt{\frac{2\pi}{r}}\frac{G}{1+\kappa} \right).$$

In the case of an *anisotropic* material, after substitution $\alpha = \pm\pi$ in the equation (7), we obtain the expressions for displacement jumps on the crack banks:

$$[[\mathbf{u}]] = \sqrt{\frac{2r}{\pi}}[\mathbf{B}]\{\mathbf{K}\}, \tag{10}$$

where $[[\mathbf{u}]] = \left\{ \begin{array}{l} \left[u_y(r,\pi) - u_y(r,-\pi) \right] \\ \left[u_x(r,\pi) - u_x(r,-\pi) \right] \\ \left[u_z(r,\pi) - u_z(r,-\pi) \right] \end{array} \right\}$ is the displacement vector of crack banks, $\{\mathbf{K}\} = \left\{ \begin{array}{l} K_I \\ K_{II} \\ K_{III} \end{array} \right\}$

is the vector of SIFs, $[\mathbf{B}] = \begin{pmatrix} \mathrm{Re}\left(\dfrac{\mu_1^{'}p_2 - \mu_2^{'}p_1}{\mu_1^{'} - \mu_2^{'}}i \right) & \mathrm{Re}\left(\dfrac{p_2 - p_1}{\mu_1^{'} - \mu_2^{'}}i \right) & 0 \\ \mathrm{Re}\left(\dfrac{\mu_1^{'}q_2 - \mu_2^{'}q_1}{\mu_1^{'} - \mu_2^{'}}i \right) & \mathrm{Re}\left(\dfrac{q_2 - q_1}{\mu_1^{'} - \mu_2^{'}}i \right) & 0 \\ 0 & 0 & \dfrac{1}{\sqrt{C_{44}^{'}C_{55}^{'} - C_{45}^{'2}}} \end{pmatrix}$ is the 3×3

matrix of the mutual influence of three components of the vector of relative displacement of the crack banks on three stress intensity coefficients. The result of inversion (10) makes it possible to calculate the SIF through the displacement of the crack banks in the case of an anisotropic material [26]:

$$\{\mathbf{K}\} = \lim_{r\to 0}\left(\frac{1}{2}\sqrt{\frac{\pi}{2r}}[\mathbf{B}]^{-1}[[\mathbf{u}]] \right), \tag{11}$$

where

$$[\mathbf{B}]^{-1} = \begin{pmatrix} \dfrac{1}{\det[\mathbf{D}]}\mathrm{Re}\left(\dfrac{\mu_1' p_2 - \mu_2' p_1}{\mu_1' - \mu_2'} i\right) & \dfrac{1}{\det[\mathbf{D}]}\mathrm{Re}\left(-\dfrac{p_2 - p_1}{\mu_1' - \mu_2'} i\right) & 0 \\[4mm] \dfrac{1}{\det[\mathbf{D}]}\mathrm{Re}\left(-\dfrac{\mu_1' q_2 - \mu_2' q_1}{\mu_1' - \mu_2'} i\right) & \dfrac{1}{\det[\mathbf{D}]}\mathrm{Re}\left(\dfrac{q_2 - q_1}{\mu_1' - \mu_2'} i\right) & 0 \\[4mm] 0 & 0 & \sqrt{C_{44}' C_{55}' - C_{45}'^2} \end{pmatrix}, \qquad (12)$$

$$\det[\mathbf{D}] = \begin{vmatrix} \mathrm{Re}\left(\dfrac{\mu_1' p_2 - \mu_2' p_1}{\mu_1' - \mu_2'} i\right) & \mathrm{Re}\left(\dfrac{p_2 - p_1}{\mu_1' - \mu_2'} i\right) \\[4mm] \mathrm{Re}\left(\dfrac{\mu_1' q_2 - \mu_2' q_1}{\mu_1' - \mu_2'} i\right) & \mathrm{Re}\left(\dfrac{q_2 - q_1}{\mu_1' - \mu_2'} i\right) \end{vmatrix}. \qquad (13)$$

It should be noted, that if the crack coordinate system does not coincide with the axes of anisotropy of the material, then the constants of the compliance and stiffness matrix must be converted into the crack coordinate system. In the case of the coordinate system rotation, the transition matrix in the plane by rotation on an angle φ has the form: $Q = \begin{pmatrix} \cos\varphi & -\sin\varphi & 0 \\ \sin\varphi & \cos\varphi & 0 \\ 0 & 0 & 1 \end{pmatrix}$

and converting elements of the compliance and stiffness tensor from the global to the crack coordinate system is defined by relations: $S_{ijkl}' = Q_{im} Q_{jn} Q_{ko} Q_{lp} S_{mnop}$, $C_{ijkl}' = Q_{im} Q_{jn} Q_{ko} Q_{lp} C_{mnop}$. In equations (10) and (11) the displacements also should be converted to the coordinate system associated with the crack: $u_i' = Q_{im} u_m$. Formulas (9)-(13) were implemented in the finite element program PANTOCRATOR [21].

Results of SIFs computations

The influence of various factors, such as: the material anisotropy, the number of edge cracks, and the distance from crack tip to the free boundary on SIFs is investigated. For this purpose, four boundary value problems with various crack configurations described in Section 2 (see Figs. 1-4) were considered.

In the *first* problem (Fig. 1) the relative distance from crack tip to free boundary a/L varied from 1 to 10.5, where L is the crack length, a is the distance from the left (right) crack tip to the left (right) plate boundary. The height of the plate H was chosen to be large enough to ignore the influence of the upper and lower boundaries. Figure 5 shows a finite element model for the problem with a single central horizontal crack for the case $a/L = 4$. The number of degrees of freedom is 185 000. The eight-node isoparametric finite elements with second order approximation are used in computations.

In order to validate the results, the finite element solution for the case $a/L = 10.5$ was compared with the analytical solution for an infinite plate (1).The practical convergence of the numerical solution on various nested meshes was investigated (for the isotropic material). When the number of degrees of freedom decreases by a factor of 2, the result changes by less than 1 %.

When varying the distance a from the crack tip to the free edge of the plate (jumper size), the finite element mesh around the crack tip was not changed, only the plate dimensions were changed. The enlarged sections were divided proportionally to the length.
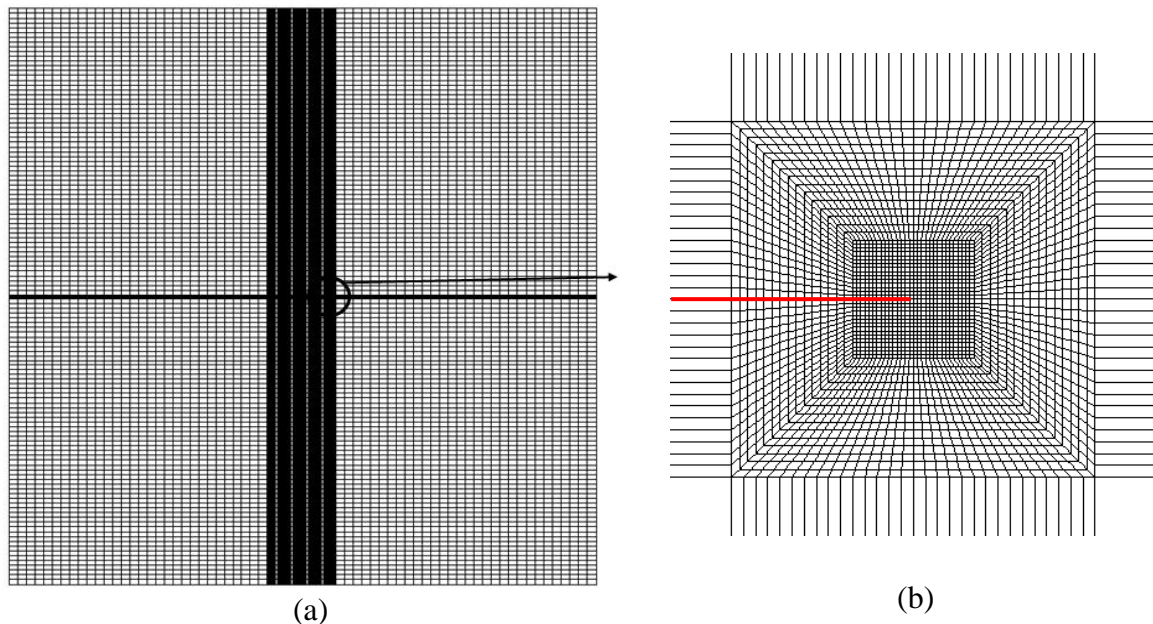
Fig. 5. Finite element model of (a) the plate with single internal horizontal crack ($a/L = 4$), (b) the vicinity of the right crack tip.

In the *second* (Fig. 2), *third* (Fig. 3) and *fourth* (Fig. 4) problems the relative distance from crack tip to free boundary a/L varied from 2 to 40, where L is the equal length of all cracks, a is the distance from the crack tip to the right boundary of plate. The plate has square shape for the problems with one and two edge cracks, whereas the plate was rectangular in the problem with three edge cracks. The distance between cracks d is equal to L. Finite element models for second, third and fourth boundary problems with edge cracks are shown in Fig. 6.

In order to validate the results, the finite element solution for the case with maximal relation $a/L = 40$ was compared with the analytical solution for single edge crack (2), two edge cracks (3) and three edge cracks (4) in an infinite plate under tension. The practical convergence of the numerical solution on various nested meshes for this problem was investigated (for the isotropic material). Difference between analytical and numerical solutions is less 0.6 % for all considered problems. Verification results are shown in Table 2.

Table 2. Verification of numerical results for the problems of uniaxial tension of plate with crack(s) from the isotropic material on the base of analytical solutions (1)-(4)

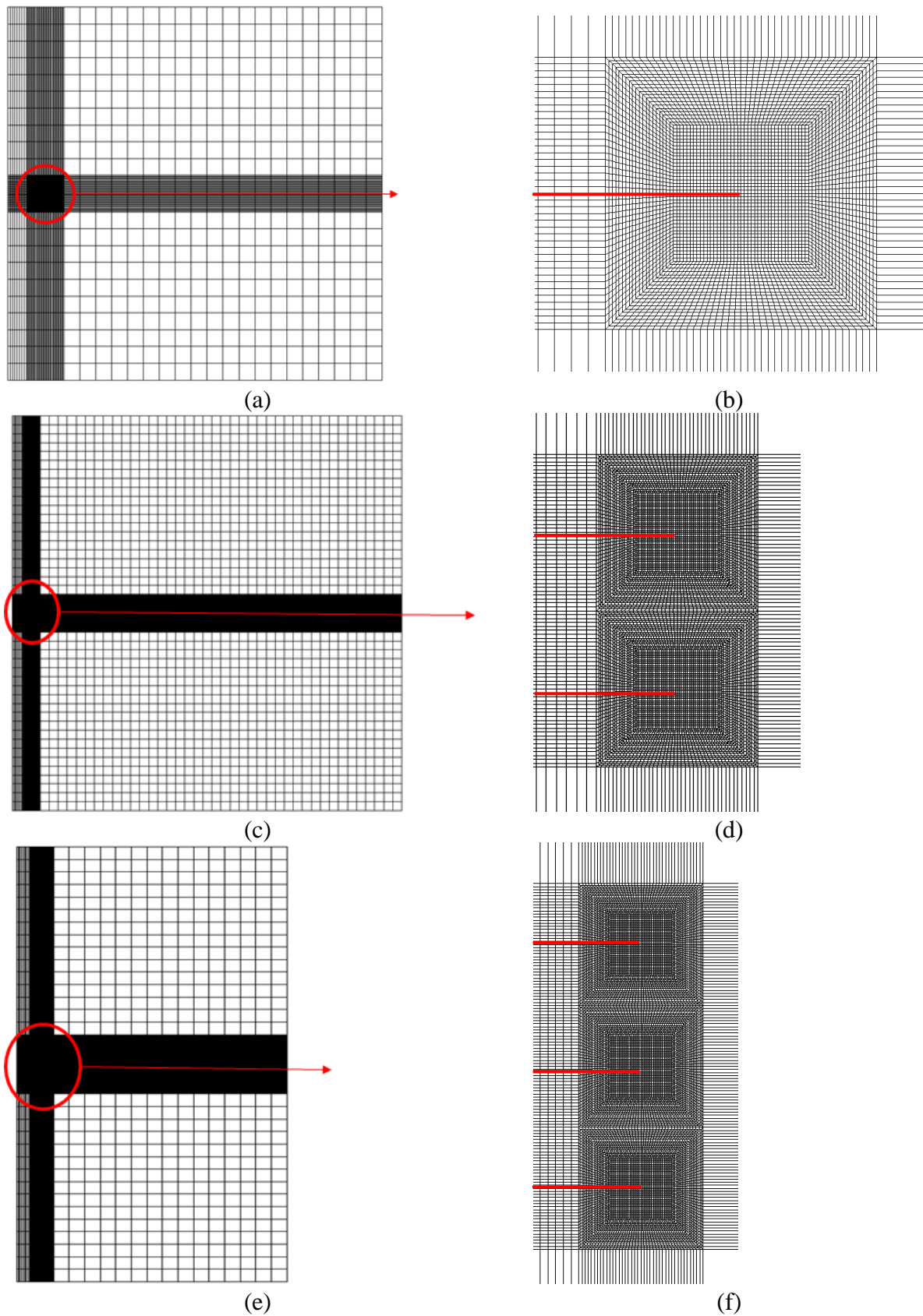|	Numerical value K_{IA}, MPa$\sqrt{m}$	Analytical value K_{IA}, MPa$\sqrt{m}$	Numerical value K_{IB}, MPa$\sqrt{m}$	Analytical value K_{IB}, MPa$\sqrt{m}$	Maximum error, %
Problem with single internal crack	124.80	125.30	124.80	125.30	0.56
Problem with single edge crack	198.57	198.51	------	------	0.03
Problem with two edge cracks	151.18	151.36	151.20	151.36	0.12
Problem with three edge cracks	143.71	144.45	104.08	104.57	0.50

Fig. 6. Finite element models for problems:
(a) *single* edge crack in a plate, (b) crack tip vicinity for *single* edge crack,
(c) *two* edge cracks in a plate, (d) crack tip vicinity for *two* edge cracks,
(e) *three* edge cracks in plate, (f) crack tip vicinity for *three* edge cracks

The numerical results of the anisotropy effect on the interaction of crack with the free boundary and interaction between cracks are presented below. Simulations has been performed for the case of the uniaxial tension (see Figs. 1(a), 2(a), 3(a), 4(a), σ_∞ =100 MPa) and for the shear loading (Figs. 1(b), 2(b), 3(b), 4(b)). In the last case the displacements on the edges of the plate are chosen to make far shear stress τ_∞ =100 MPa.

Figure 7 shows of the anisotropy influence on SIFs for the *first* problem concerning the *internal crack* in the plate under tension (Fig. 7(a)) and shear loading (Fig. 7(b)). In the first loading case, the pure I fracture mode is realized, and in the second case the pure II fracture mode takes place. For ease of comparison of results for cracks with different relative lengths, all curves are scaled to the isotropic solution.
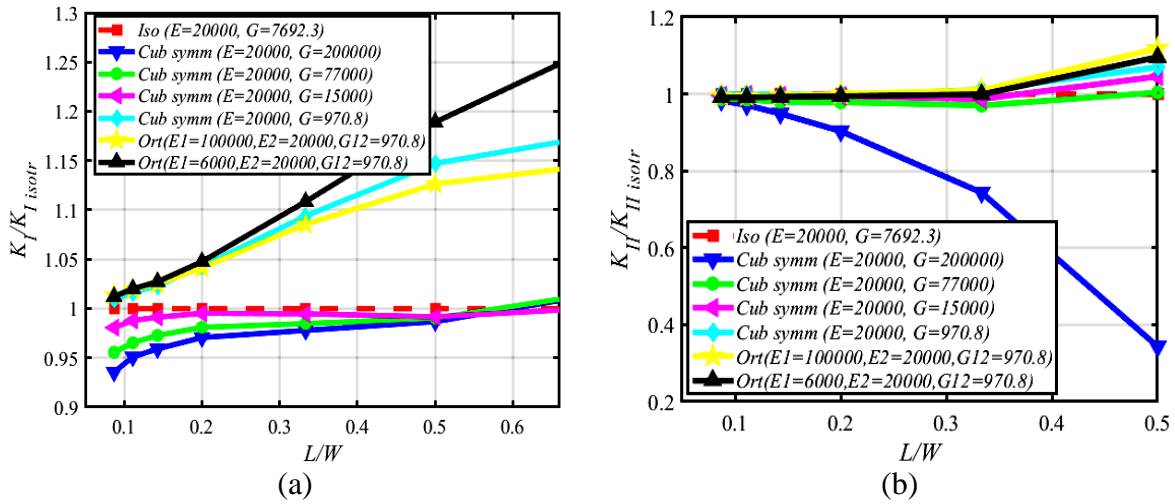

Fig. 7. Influence of anisotropy on SIF for internal crack in the plate under
(a) tension (I fracture mode), and (b) shear (II fracture mode)

It should be noted that influence of anisotropy is higher when the internal crack is close to free boundaries. Influence for shear loading is stronger in several times than for the tension loading. A possible explanation is that the shear modulus G for an anisotropic material varies over a wide range. Note, that all curves are obtained at equal values of Young's modulus E = 20000 MPa in the vertical direction. Away from free edges (L/W<0.1), the shear crack (unlike tensile crack) is almost insensitive to the type of anisotropy.

Note, depending on the elastic moduli, SIFs for an anisotropic material can be larger or smaller than the SIFs for an isotropic material.

Figure 8 shows the anisotropy influence on SIFs for the *second* problem concerning the *single edge crack* in the plate under tension (Fig. 8(a), pure I fracture mode) and shear loading (Fig. 8b, the pure II fracture mode).

The dependences of $K_I (L/W)$ / $K_{I\,isotr}$ under tension are not monotonic (Fig. 8(a)), while $K_{II} (L/W)$ / $K_{II\,isotr}$ under shear are monotonic (Fig. 8(b)). A possible explanation that dependence $K_{II} (L/W)$ / $K_{II\,isotr}$ under shear are monotonic is varied shear modulus G. A possible explanation that dependence $K_I (L/W)$ / $K_{I\,isotr}$ under tension for cubic symmetry and orthotropic materials are not monotonic, is that we varied plate dimensions over a wide range and influence of shear modulus G and effect of free boundary are competing effects.
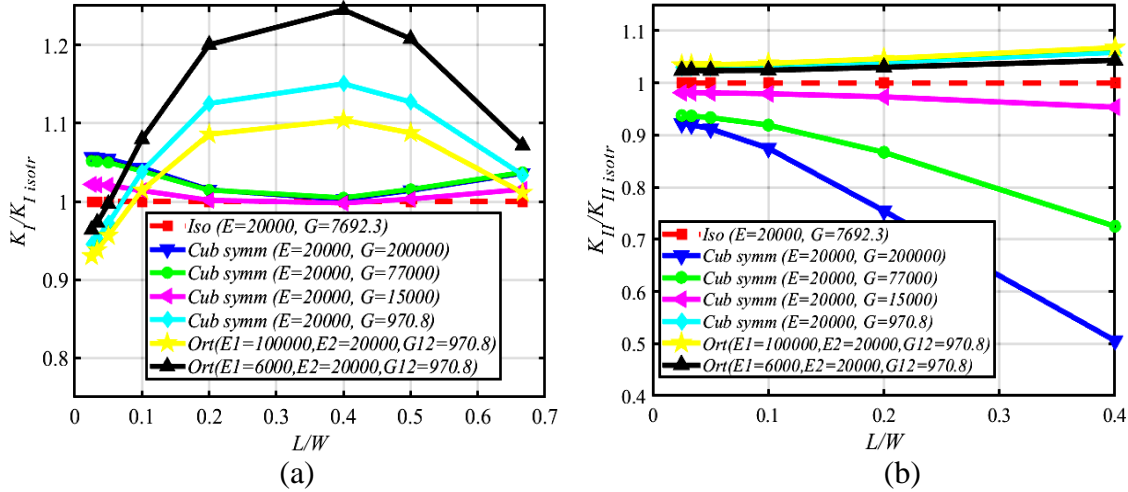
Fig. 8. Influence of anisotropy on SIF for single edge crack in the plate under
(a) tension (I fracture mode), and (b) shear (II fracture mode)

However, the material anisotropy strongly affects the SIFs in all cases considered. Influence of material anisotropy is monotonously increase when closing to free boundary for II fracture mode. Also the influence for II fracture modes is stronger in several times than for I fracture modes. A possible explanation is that the shear modulus G for an anisotropic material varies over a wide range. The main difference between edge and internal cracks is the alternative nature of the effect of anisotropy away from the free edges ($L/W<0.1$). As the crack approaches the free surface ($L/W \rightarrow 1$), the same pattern of anisotropy effects is observed.

Figure 9 shows the anisotropy influence on SIFs for the *third* problem concerning the *two edge cracks* in the plate under tension (Fig. 9(a)) and shear loading (Fig. 9(b)). Due to the influence of cracks on each other, pure fracture modes (in contrast to the first and second problems) are not realized neither in tension nor in shear. Both K_I and K_{II} are different from zero and a mixed fracture mode is realized.
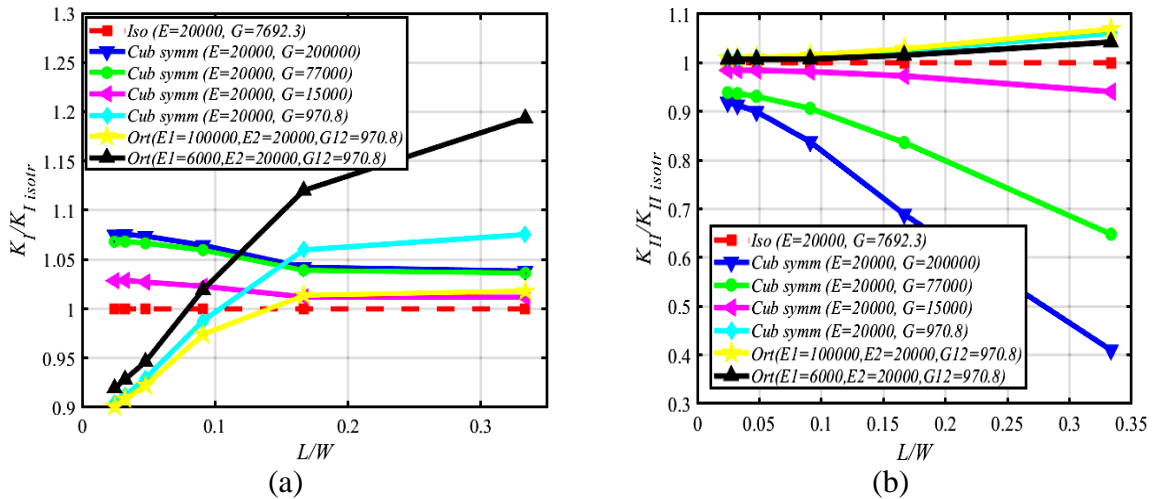

Fig. 9. Influence of anisotropy on SIF for two edge cracks in the plate under
(a) tension, and (b) shear

Influence of material anisotropy is monotonously increase when closing to free boundary for shear loading (Fig. 9(b)), while this effect is not observed in tension (Fig. 9(a)). In general, in shear, the behavior of one and two edge cracks is quite similar (cf. Figs. 8(b) and 9(b)).

In tension, the behavior of one and two edge cracks for cubic symmetry is also very close (cf. Figs. 8(a) and 9(a)), while significant differences are observed for orthotropic material.

Figure 10 shows influence of anisotropy on SIFs for the *fourth* problem concerning the *three edge cracks* in the plate under tension (Fig. 10(a,b)) and shear loading (Fig. 10(c,d)). Due to the influence of cracks on each other, pure fracture modes are not realized neither in tension nor in shear loading. Both K_I and K_{II} are different from zero and a mixed fracture mode is observed. The SIFs for the central crack (with the crack tip at point B in Fig. 4) differ from the SIFs for the outermost cracks (with the crack tip at points A in Fig. 4).
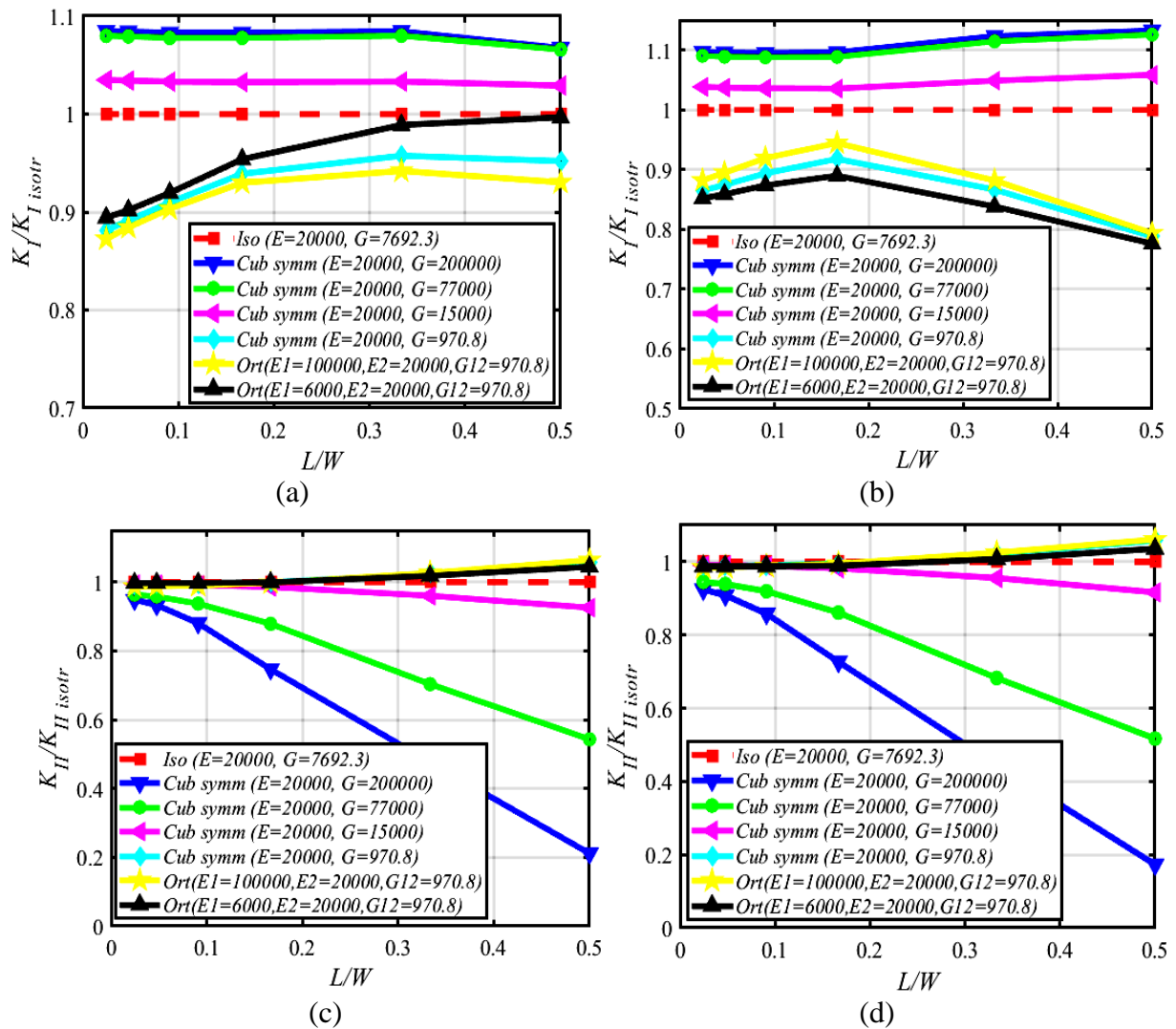

Fig. 10. Influence of anisotropy on SIFs for three edge cracks in the plate under (a) tension (Point A – outer crack), K_I, (b) tension (Point B – central cracks), K_I, (c) shear (Point A – outer crack), K_{II}, (d) shear (Point B – central crack), K_{II}

For the three edge cracks, the effect of anisotropy on the SIF is also very prominent. The character of dependences $K_I (L/W) / K_{I\,isotr}$ add $K_{II} (L/W) / K_{II\,isotr}$ for three cracks is close to the character of corresponding dependences for two cracks for cubic symmetry (cf. Figs. 10(a,b) with 9(a) and Figs. 10(c,d) with 9(b)), while significant differences are observed for orthotropic material. From the comparison of points A and B, it can be seen that the relative SIFs $K_I (L/W) / K_{I\,isotr}$ in tension are larger for the internal crack with the tip at point B, while the absolute values $K_I (L/W)$ are larger for the lateral cracks with the tip at point A, which reflects the shading effect.

Conclusions

The results of multivariant numerical experiments have demonstrated sensitivity of SIFs to material anisotropy for both internal and edge cracks under both tensile and shear loading. Depending on the elastic moduli, SIFs for an anisotropic material can be larger or smaller than the corresponding SIFs for an isotropic material. The effect of material anisotropy strongly depends on shear modulus value. For pure shear loading the influence of material anisotropy becomes stronger when the crack is approaching to the plate boundary. For uniaxial tension loading the effect of material anisotropy is approximately constant for different distances to the plate boundary in the problem of interaction of the cracks. The influence of material anisotropy in the problem with the three edge cracks is stronger than in the problem with one edge crack for purely shear loading (the increase in SIF reaches 80 %).

References

1. Shalin RE, Svetlov IL, Kachanov EB, Toloraiya VN, Gavrilin OS. *Single crystals of nickel heat-resistant alloys*. Moscow: Mashinostroenie; 1997. (In-Russian)
2. Getsov LB. *Materials and strength of gas turbine parts*. Rybinsk: Gazoturbinnye Tekhnologii; 2010. (In-Russian)
3. Dulnev RA, Kotov PI. *Thermal fatigue*. Moscow: Mashinostroenie; 1980. (In-Russian)
4. Getsov LB, Dobina NI, Rybnikov AI, Semenov AS, Staroselskii A, Tumanov NV. Thermal fatigue resistance of a monocrystalline alloy. *Strength of Materials*. 2008;40(5): 538–551.
5. Semenov AS, Semenov SG, Nazarenko AA, Getsov LB. Computer simulation of fatigue, creep and thermal fatigue cracks propagation in gas turbine blades. *Materials and Technology*, 2012; 3: 197–203.
6. Semenov AS, Semenov SG, Getsov LB. Methods for calculating the growth rate of fatigue cracks, creep and thermal fatigue in poly- and single-crystal gas turbine blades. *Journal of Strength Materials*. 2015; 2: 61–87.
7. Getsov LB, Semenov AS, Ignatovich IA. Thermal fatigue analysis of turbine discs on the base of deformation criterion. *International Journal of Fatigue*. 2017; 97: 8–97.
8. Getsov LB, Semenov AS. On the safety margins of gas turbine engine parts under thermal cyclic loading. *Aviation Engines*. 2023; 18(1): 79–98.
9. Liebowitz H. *Fracture, an Advanced Treatise. Vols. I and II.* NY: Academic Press; 1968.
10. Sih GC. (Ed.) *Mechanics of Fracture. Methods of analysis and solutions of crack problems.* Netherlands, Leyden: Noordhoff International Publishing; 1973.
11. Morozov NF. *Mathematical Problems in the Theory of Cracks.* Moscow: Nauka; 1984. (In-Russian)
12. Murakami Y. *Stress Intensity Factors Handbook.* Pergamon; 1987.
13. Kuna M. *Finite Elements in Fracture Mechanics.* New York: Springer; 2013.
14. Sih GC, Paris PC, Irwin GR. On cracks in rectilinearly anisotropic bodies. *International Journal of Fracture Mechanics.* 1965;1: 189–203.
15. Barnett DM, Asaro RJ. The fracture mechanics of slit-like cracks in anisotropic elastic media. *Journal of Mechanics and Physics of Solids.* 1972;20(6): 353–366.
16. Azhdari A, Nemat-Nasser S Experimental and computational study of fracturing in an anisotropic brittle solid. *Mechanics of Materials.* 1998;28(1-4): 247–262.
17. Savikovskii AV, Semenov AS, Getsov LB. Crystallographic orientation, delay time and mechanical constants influence on thermal fatigue strength of single-crystal nickel superalloys. *Materials Physics and Mechanics.* 2020;44(1): 125–136.
18. Savikovskii AV, Semenov AS, Kachanov ML. Influence of Material Anisotropy on the Interaction of a Crack with a Free Boundary. *Mechanics of Solids.* 2022;57: 2030–2037.
19. Yu H., Kuna M. Interaction integral method for computation of crack parameters K-T – a review. *Engineering Fracture Mechanics.* 2021;249: 107722.
20. Ozkan U, Nied HF, Kaya AC. Fracture analysis of anisotropic materials using enriched crack tip elements. *Engineering. Fracture Mechanics.* 2010;77: 1191–1202.

21. Semenov AS. PANTOCRATOR – finite-element program specialized on the solution of non-linear problems of solid body mechanics. In: *Proc. of the V-th International. Conf. "Scientific and engineering problems of reliability and service life of structures and methods of their decision"*. SPb: Izd-vo SPbGPU; 2003. p.466–480. (In-Russian)

22. Kachanov LM. *Osnovy mekhaniki razrusheniya*. Moscow: Nauka; 1974. (In-Russian)

23. Banks-Sills L, Hershkovitz I, Wawrzynek PA, Eliasi R, Ingraffea AR. Methods for calculating stress intensity factors in anisotropic materials: Part I – z = 0 is a symmetric plane. *Engineering. Fracture Mechanics*. 2005;72(15): 2328–2358.

24. Judt PO, Ricoeur A, Linek G. Crack path prediction in rolled aluminum plates with fracture toughness orthotropy and experimental validation. *Engineering Fracture Mechanics*. 2015;138: 33–48.

25. Lekhnitskiy SG. *Teoriya uprugosti anizotropnogo tela*. Moscow: Nauka; 1977. (In-Russian)

26. Ranjan S, Arakere NK. A Fracture-mechanics-based methodology for fatigue life prediction of single crystal nickel-based superalloys. *Journal of Engineering Gas Turbines Power*. 2008;130(3): 032501.

THE AUTHORS

Savikovskii A.V.
e-mail: savikovskii.artem@yandex.ru

Semenov A. S.
e-mail: Semenov.Artem@googlemail.com